

Decoding the amplitude and slope of continuous signals into spikes with a spiking point neuron model

Rebecca Miko¹, Marcus Scheunemann^{2,3}, Volker Steuber¹, and Michael Schmuker^{1,*}

¹Biocomputation Research Group, University of Hertfordshire, Hatfield, United Kingdom

²Adaptive Systems Research Group, University of Hertfordshire, Hatfield, United Kingdom

³Autonomy Department, Dexory, London, United Kingdom

*m.schmuker@herts.ac.uk

ABSTRACT

In this study, we harness the signal processing potential of neurons, utilizing the Izhikevich point neuron model to efficiently decode the slope or amplitude of fluctuating continuous input signals. Using biophysically detailed compartmental neurons often requires significant computational resources. We present a novel approach to create behaviours and simulate these interactions in a lower-dimensional space, thereby reducing computational requirements. We began by conducting an extensive search of the Izhikevich parameter space, leading to the first significant outcome of our study: i) the identification of optimal parameter sets for generating slope or amplitude detectors, thereby achieving signal processing goals using neurons. Next, we compared the performance of the slope detector we discovered with a biophysically detailed two-compartmental pyramidal neuron model. Our findings revealed several key observations: ii) bursts primarily occurred on the rising edges of similar input signals, iii) our slope detector exhibited bi-directional slope detection capabilities, iv) variations in burst duration encoded the magnitude of input slopes in a graded manner. Overall, our study demonstrates the efficient and accurate simulation of dendrosomatic behaviours. Real-time applications in robotics or neuromorphic hardware can utilize our approach. While biophysically detailed compartmental neurons are compatible with such hardware, Izhikevich point neurons are more efficient. This work has the potential to facilitate the simulation of such interactions on a larger scale, encompassing a greater number of neurons and neuronal connections for the same computational power.

Introduction

There is a wide range of approaches to modelling neuronal activity. Single-neuron models are often required to reproduce very specific features of existing experimental data, e.g. replicating the bursting mechanisms and gradient detection of Pyramidal neurons¹. Often these models represent known biophysical mechanisms in compartments, such as the pyramidal neuron model which combines the soma and axon in one compartment and the dendritic region in another, forming a two-compartmental model. These spatially complex models are usually focused on the computational aspects of the information processing within the neuron, prioritizing accuracy and biological realism rather than efficiency. However, in various research fields like gas-based navigation in robotics, there is a need for less computationally expensive models that efficiently process information, particularly amplitude and slope detectors.

Amplitude and slope are important dynamical features of sensory signals, encoding information about the scene²⁻⁴. The instantaneous dynamics of gas concentration in a turbulent plume are extremely complex^{2,5}, and this rich temporal structure and spatial distribution of gas plumes demand rapid⁵⁻⁷, low-latency responses to temporal cues in these signals. We created a neuron from the Izhikevich⁸ point neuron model, which inherently processes information with less computation in lower-dimensional space. We demonstrate how this neuron model can mimic the behaviours from the biophysically detailed two-compartmental pyramidal neuron model¹ without compromising accuracy.

Izhikevich⁸ maintained an effective trade-off between the biological plausibility of Hodgkin-Huxley-type dynamics and the computational efficiency of integrate-and-fire neurons, making it a popular choice for implementing neuronal computations onto neuromorphic hardware⁹⁻¹¹ and robotic platforms^{12,13}. Izhikevich presented a two-dimensional system of ordinary differential equations (Eq. 1) with an auxiliary after-spike reset (Eq. 2). The parameters in the equations map to known biological features of neuronal spiking processes.

The dimensionless variables, membrane potential (v) and recovery variable (u), represent the core elements of the model. The parameters (a , b , c , d) control the recovery rate of u , sensitivity of u , after-spike reset of v , and after-spike reset of u , respectively. The model's mathematical simplicity, with only one non-linear term (v^2), contributes to its computational efficiency.

$$\begin{aligned} v' &= 0.04v^2 + 5v + 140 - u + I \\ u' &= a(bv - u) \end{aligned} \quad (1)$$

$$\text{if } v \geq 30\text{mV, then } \begin{cases} v \leftarrow c \\ u \leftarrow u + d \end{cases} \quad (2)$$

While the Izhikevich model does not capture specific biophysical mechanisms or the spatial complexity of neurons, it has demonstrated the ability to replicate various types of known neural behaviours, including intrinsically bursting and fast-spiking. In our study, we compare a bursting slope-detecting neuron, that we created using the Izhikevich model, with the two-compartmental biophysical neuron model¹. It has been reported¹⁴ that pyramidal neurons detect temporal changes (slope) and frequently firing short bursts of high frequency. The model includes a dendrite compartment with persistent sodium and slow potassium currents responsible for bursting behaviour, while the somatic region contains Hodgkin-Huxley-type¹⁵ currents that generate fast spikes.

Through simulations with sinusoidal and naturalistic input currents, the biophysical neuron model investigates the temporal features triggering bursting behaviour and suggests that the neuronal output depends more on the slopes of the input signal than the amplitudes. If the neuron we propose exhibits comparable behaviour (which we later show to be the case), it could offer an efficient and accurate means of simulating dendrosomatic behaviours.

Results

We present the results from our search of the Izhikevich parameter space and analyse their implications. We show how we located the optimal sets to create the strongest slope and amplitude detectors and test for the neuron's robustness. We then present the results from our three-part comparison study, where we compared the Izhikevich bursting slope detector neuron we discovered to a biophysically detailed two-compartmental pyramidal neuron model¹. The results were carefully displayed to enable a side-by-side comparison with the results from the biophysical neuron model, including the analysis.

i) Identifying slope and amplitude detectors in the Izhikevich parameter space

In this section, we present the results of our search for optimal detectors in the Izhikevich parameter space. We show three identical grids that cover a wide range of values for the parameters a , c , and d .

A rectified sinusoidal input signal with a frequency of 4 Hz was injected into each Izhikevich point neuron using the defined parameters. The spike trains were extracted and compared to the original input signal to determine the features that triggered the neuron's response. We specifically looked at the spike rate corresponding to the rising edges of the input signal to identify slope detectors and the spike rate corresponding to the peaks of the input signal to identify amplitude detectors. Later, we investigated whether there was a relationship between these detectors and the bursting mechanisms, producing the third grid in these results.

The grids display the *slope detection percentage*, *amplitude detection percentage*, and *bursting percentage* for each parameter combination. For instance, a neuron with a 100 % *amplitude detection percentage* only spikes on the peaks of the input signal.

Fig. 1a shows the grid for slope detection. We observed that low values of parameter a , particularly with higher c values (such as $c = -35$), produces strong slope-detecting behaviour. This pattern was consistently observed across various regions of the grid. Additionally, the grid suggests that the parameter d should not be set too low, as doing so resulted in neurons exhibiting 0 % slope detection in certain regions of the map. Based on these observations, we selected the neuron with parameters $\{a:0.01, b:0.2, c:-35, d:5.0\}$ as an example slope detector (Fig. 1b). This neuron configuration was chosen based on its strong slope-detecting capabilities demonstrated in our analysis.

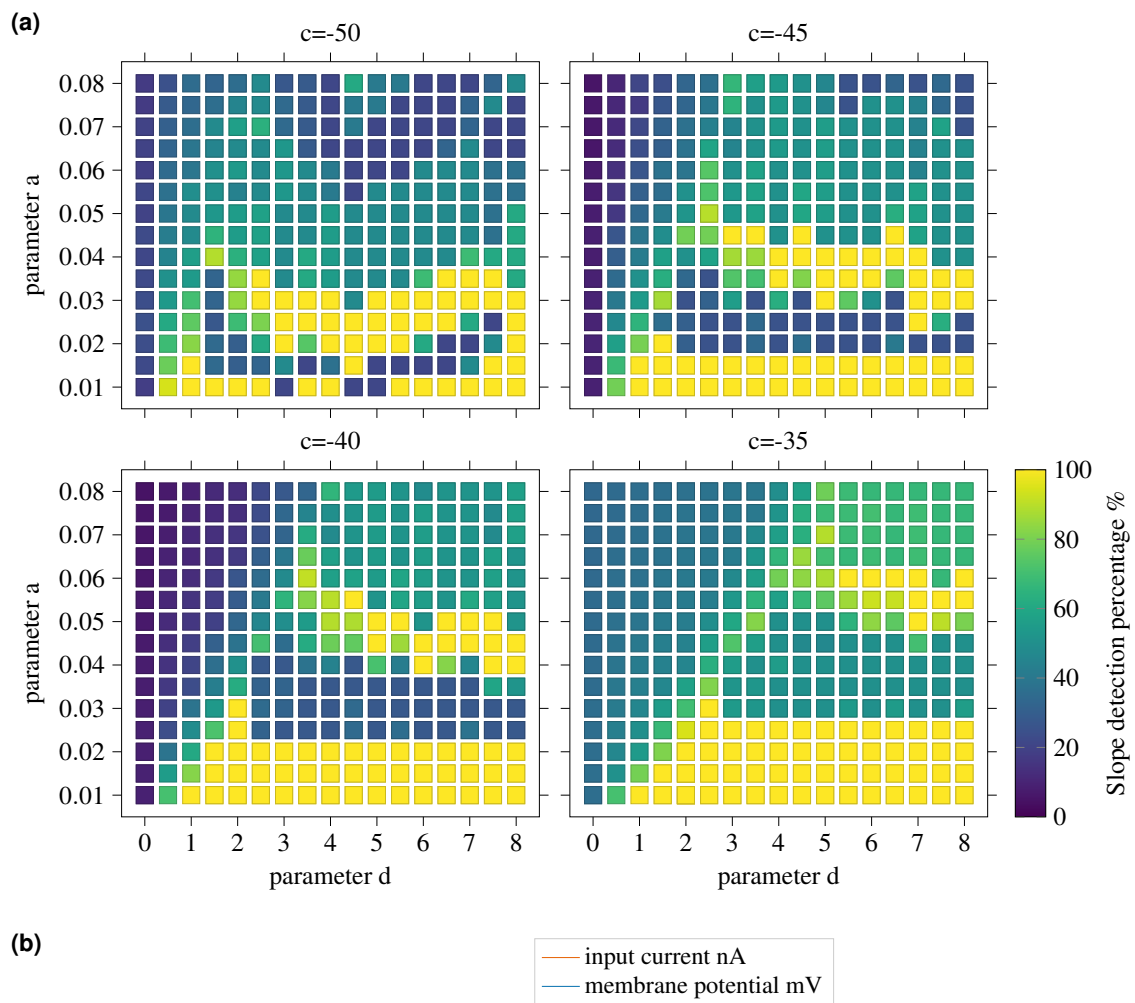


Figure 1. *Top panel:* results of the search for parameter combinations that enable slope-detection; Izhikevich parameters d (x-axis), a (y-axis), and c (panels). The slope-detection capability is confined to specific regions in parameter space. The *slope detection percentage* highlights the regions that generate strong slope detectors (yellow). *Bottom panel:* comparison of a slope detector we discovered with parameters $\{a:0.01, b:0.2, c:-35, d:5.0\}$ and a rectified segment of the 4 Hz sinusoidal input signal. A burst of spikes on the rising flank illustrates the slope-detection behaviour for which the neuronal parameters have been optimized.

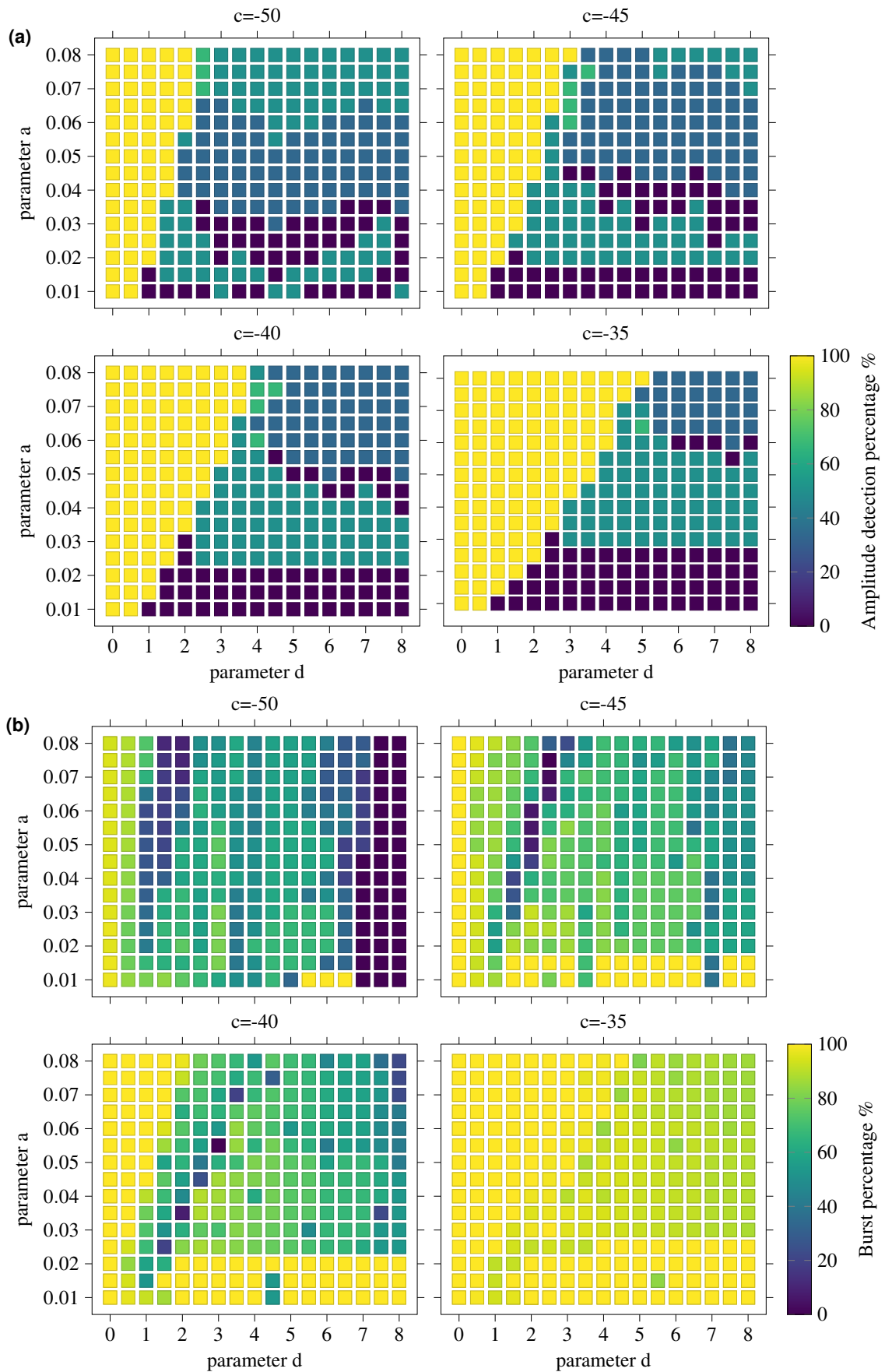


Figure 2. Results from search of Izhikevich parameters d (x-axis), a (y-axis), and c . Yellow regions indicate strong *top panel*: amplitude detectors; *bottom panel*: bursting behaviour (inter-spike interval ≤ 10 ms).

Fig. 2a shows the grid for amplitude detection. We observed that lower values of d combined with higher a values produces strong amplitude-detecting behaviour. Higher c values also generated a larger area of amplitude-detecting neurons. This was observed in the slope detector grid (Fig. 1a), suggesting a commonality with the membrane voltage reset.

Comparing the slope detector grid (Fig. 1a) and the amplitude detector grid (Fig. 2a) reveals cases where a set of parameters can produce both slope and amplitude-detecting neurons. For instance, the neuron with parameters $\{a:0.04, b:0.2, c:-35, d:5.0\}$ exhibits a *slope detection percentage* and an *amplitude detection percentage* of 50 %, indicating that it spikes on both the rising edges and peaks of the signal.

Fig. 2b shows the grid for bursting behaviour. It shows that higher c values generally lead to bursting neurons. The highest explored value (i.e., $c = -35$) produced neurons that were almost always bursting. The combination of parameters a and d also affects the bursting mechanisms, with higher values of both leading to a decrease in the *burst percentage*. Furthermore, we observed no strong relationship between the bursting grid (Fig. 2b) and the slope (Fig. 1a) and amplitude (Fig. 2a) detector grids.

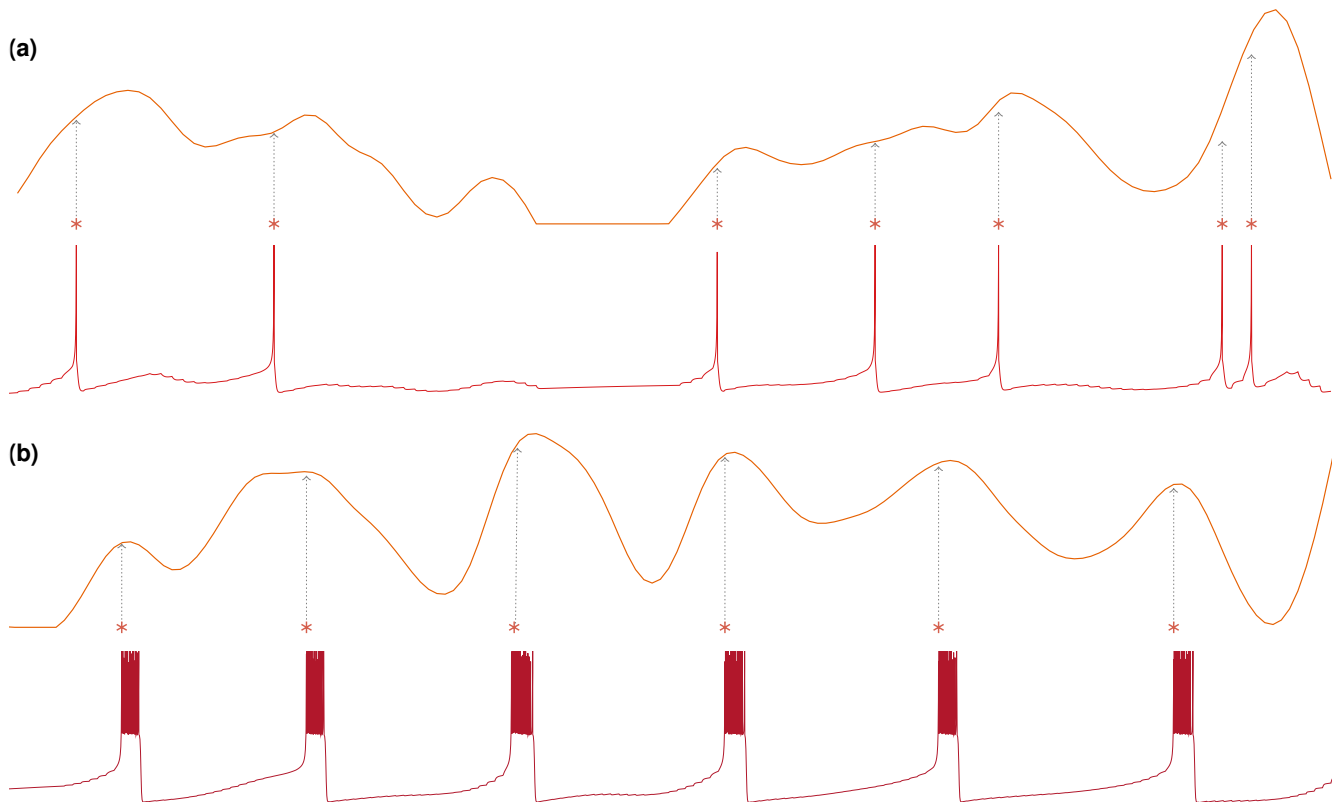


Figure 3. *Top trace:* Gaussian white noise input nA (5 Hz; $\mu = .006$; $\sigma = .015$). *Bottom trace:* membrane potential mV response. *Top panel:* the neuron has parameters $\{a:0.01, b:0.2, c:-50, d:8.0\}$. Asterisks mark spikes (grey dotted lines added for clarity). *Bottom panel:* neuron has parameters $\{a:0.05, b:0.2, c:-40, d:1.0\}$. Asterisks mark burst onsets. Bursts ($ISI \leq 10$ ms) occur on the peaks of the current. No single spikes were produced.

Fig. 3a demonstrates an example of a slope detector without the bursting mechanism. This neuron, with parameters $\{a:0.01, b:0.2, c:-50, d:8.0\}$, is one of the strongest slope detectors, with a *slope detection percentage* of 100 %, and simultaneously one of the weakest bursting neurons with a *burst percentage* of 0 %. We tested its robustness by injecting Gaussian white noise input (5 Hz; $\mu = 0.006$; $\sigma = 0.015$). We show that the spike rate alone can indicate input slopes and that the detector is not limited to sinusoidal input signals.

Finally, we present the output from one of the amplitude detectors and demonstrate its robustness by injecting a similar signal. This time, we demonstrate a neuron with an *amplitude detection percentage* of 100 % and *burst percentage* of 100 %. Fig. 3b shows that the detector bursts preferentially at signal peaks.

ii) Bursting slope detector comparison

In our comparison study, we conducted experiments to compare the bursting slope detector neuron we discovered with the biophysical neuron model proposed by Kepecs et al.¹. This model features a dendrite compartment that facilitates bursting

behaviour and a somatic region that produces fast spikes. For a fair comparison, we developed a robust neuron that achieved a 100 % *slope detection percentage* and a 100 % *burst percentage*. We generated similar input signals and analyzed the output responses to evaluate the performance of the detector.

The first result of our comparison study is shown in Fig. 4a, where we plotted the membrane potential response of the bursting slope detector neuron to a Gaussian white noise input signal (5 Hz; $\mu = .008$; $\sigma = .015$). The bursting slope detector neuron successfully mimicked the biophysical neuron model's ability to signal consecutive up-strokes without intervening down-strokes. However, we observed that the detector we discovered produced a cleaner and more efficient output, as there were no isolated spikes present.

Furthermore, we analysed the response of the bursting slope detector to stimulus up-strokes at different frequencies. The Spike-triggered Average (STA) plot was used to identify the features of the input signal triggering its response. Fig. 4b demonstrates that this detector is capable of responding to stimulus up-strokes across a wide range of frequencies, similar to the behaviour observed in the biophysical neuron model.

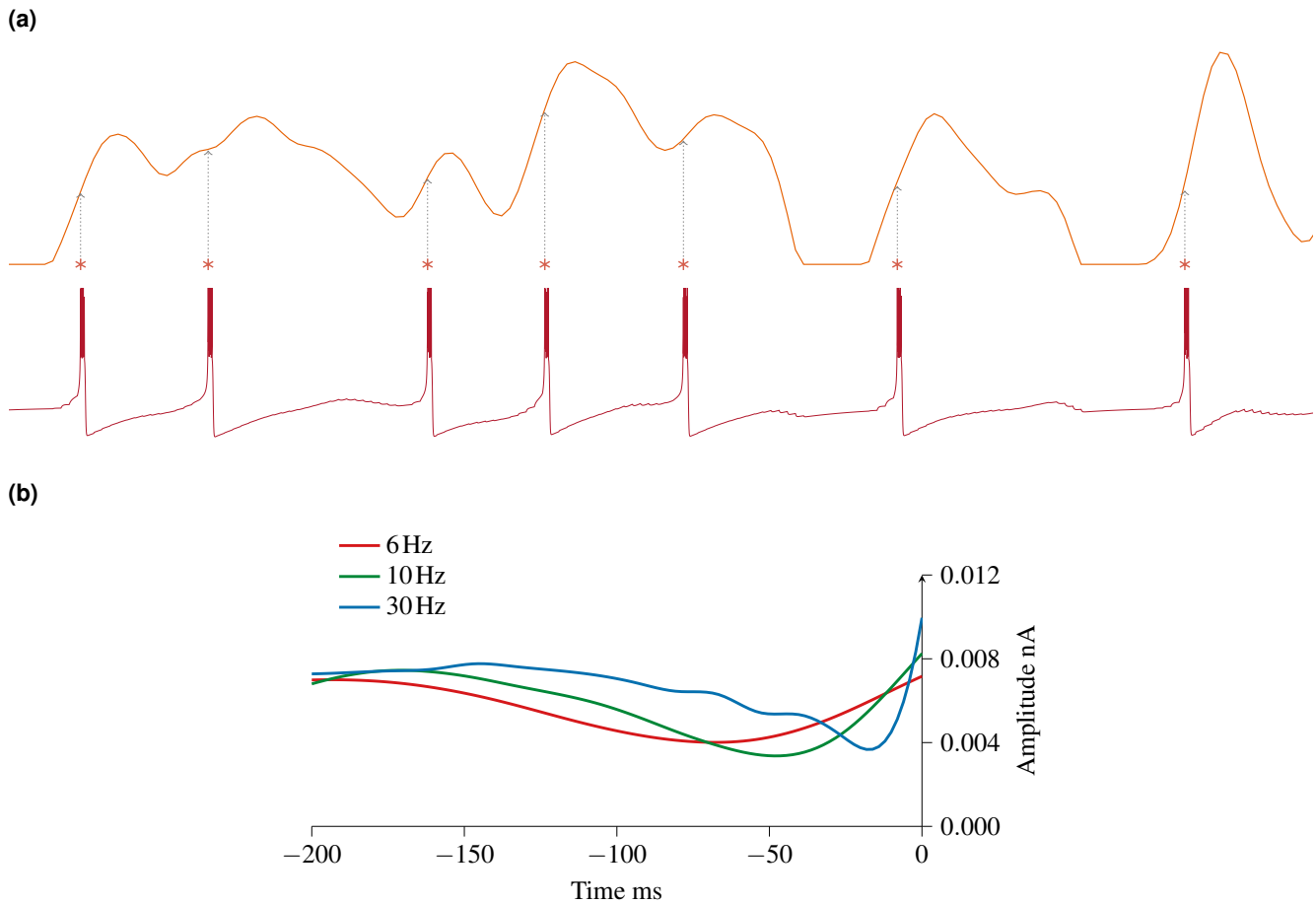


Figure 4. *Top panel:* response of the neuron with parameters $\{a:0.01,b:0.2,c:-35,d:5.0\}$. *Top trace:* Gaussian white noise input nA (5 Hz; $\mu = .006$; $\sigma = .015$). *Bottom trace:* membrane potential mV response. Asterisks mark burst onsets (grey dotted lines added for clarity). Bursts ($ISI \leq 10$ ms) occur on the rising edge of the current. No single spikes were produced. *Bottom panel:* spike-triggered Average (STA) showing features of the input that triggered bursts at different frequencies. The results demonstrate that the bursting slope detector neuron we discovered follows stimulus up-strokes over a wide range of frequencies.

iii) Bi-directional slope detection

We present our second result of the comparison study of the bursting slope detector neuron we discovered to the biophysical neuron model¹, specifically to determine whether the slope-detector was capable of bi-directional slope detection.

The results revealed that bursts occurred on the up-strokes of the signal (*e neuron*) and on the down-strokes of the inverted signal (*i neuron*), as demonstrated in Fig. 5, thereby showing that the slope detector was capable of bi-directional slope detection.

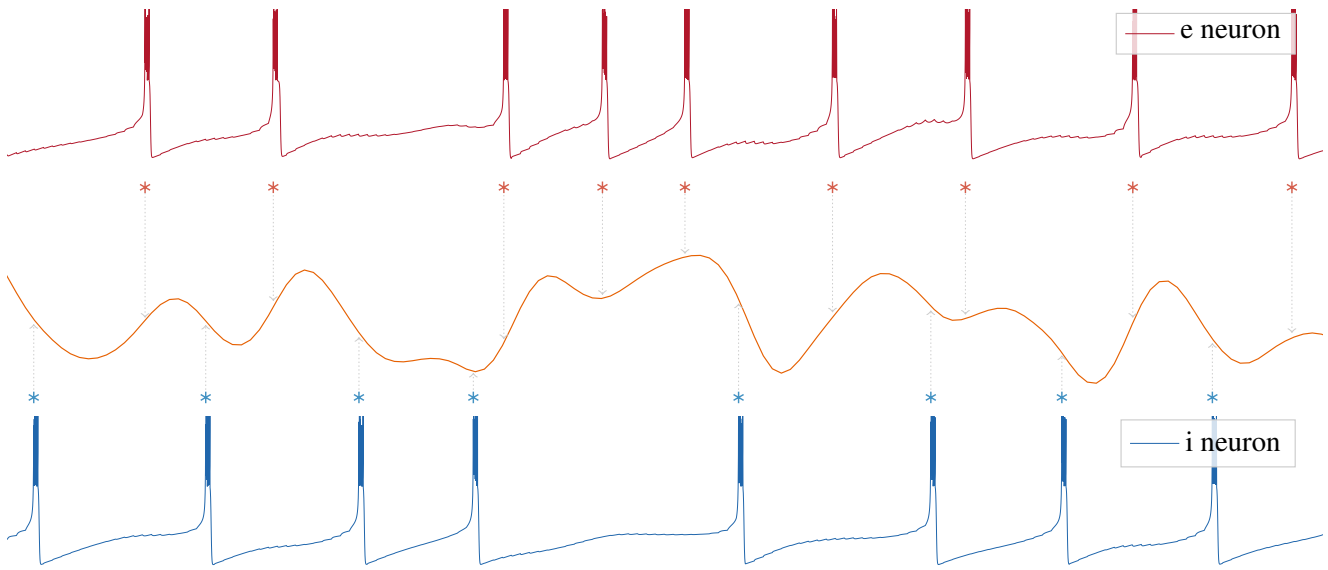


Figure 5. *Middle trace:* input current nA (5 Hz; $\mu = .008$; $\sigma = .015$). *Top trace:* membrane potential mV response from *e neuron*. *Bottom trace:* membrane potential mV response from *i neuron*, where the *middle trace* was inverted. Asterisks mark burst onsets (grey dotted lines added for clarity).

iv) Burst duration encoding

We present our final results from the comparison study, where we investigated whether the slope detector signalled the slope magnitude. In this case, we increased the variable a from 0.01 to 0.06, resulting in the neuron producing bursts of 7 or 8 spikes ($B7$, $B8$ in Fig. 6a). The KED plot shows the number of spikes per burst compared to the slopes of the input signal. These burst durations corresponded to different slope magnitudes with little overlap, as indicated by AUC value of 0.97 for the ROC curve in Fig. 6b.

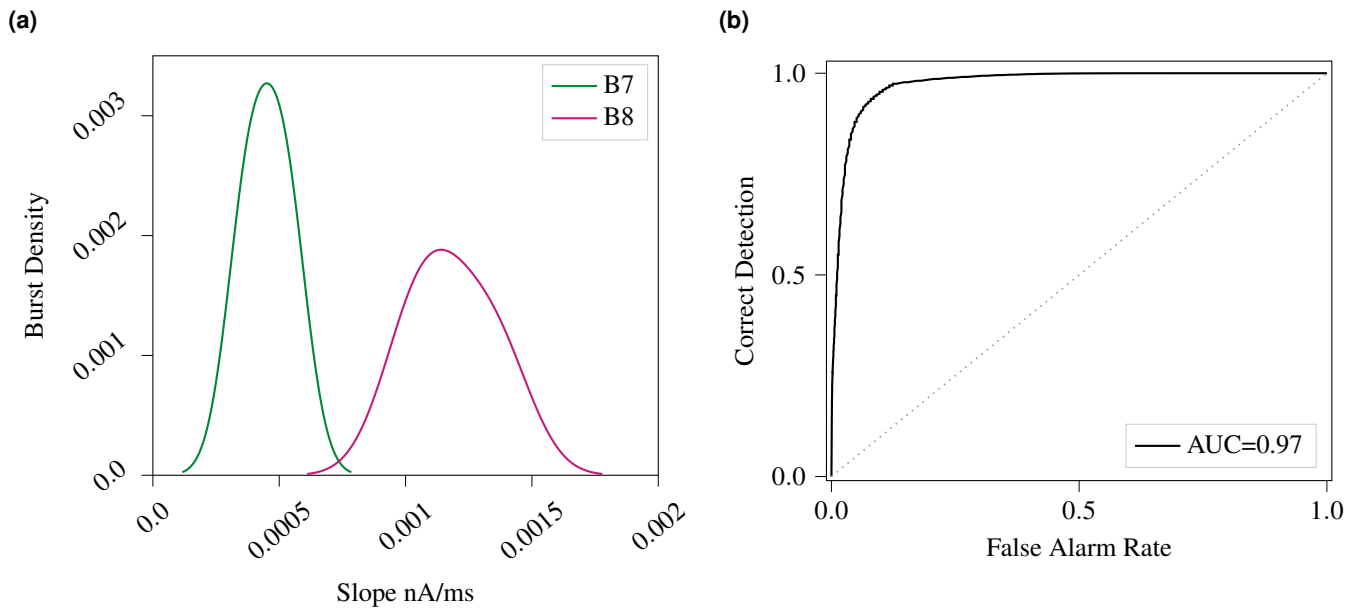


Figure 6. *Left:* distributions of input slopes for bursts durations, where the point neuron with parameters $\{a:0.06, b:0.2, c:-35, d:5.5\}$ produces 7- or 8-spike bursts. *Right:* receiver operator characteristics (ROC) curve showing discriminability of 7- and 8-spike burst distributions (from Fig. 6a). The area under the curve (AUC) value is included for clarity.

The results revealed that the detector not only marked the occurrences of slopes in the signal but also encoded the magnitude of input slopes in a graded manner through the length of bursts.

Discussion

The main aim of this work was to create a neuron which exhibits a processing necessity. Our study provides valuable insights into the creation of amplitude and slope-detecting neurons with computational efficiency. We identified sets of model parameters that enable neurons to signal the rate of change in an input signal, while being minimally affected by its absolute value. Such behaviour could be useful e.g. to implement a high-pass filter with model neurons in a neuromorphic signal processing context, moving beyond the sole goal of mimicking biological observations.

Such slope-detecting neurons could be applied to various fields of research, for example, gas-based navigation in robotics. Amplitude and slope are important dynamical features of sensory signals, encoding information about the scene²⁻⁴. The ability to detect both up-strokes and down-strokes of the input signal enables potential applications in gas-based navigation research^{3,5,16,17}, where detecting the presence and absence of gas provides valuable information about the olfactory scene. The ability of the model to report the magnitude of input slopes in a graded manner through the length of bursts produced further supports an application in gas-based navigation studies, where the duration of slope durations can inform the distance to an odour source³.

Sensor devices that can very quickly respond to temporal cues in these signals are a prerequisite to decode information encoded in rapid concentration fluctuations⁵⁻⁷. Power-economic electronic olfaction devices have been demonstrated that can resolve temporal dynamics of stimulus intensity with sub-second precision¹⁸. They are portable and function in uncontrolled natural environments¹⁹, paving the way for an application in robotics, in particular in combination with neuromorphic computing. A spiking electronic olfaction device capable of high temporal resolution has been described²⁰. Spike trains from such devices could be fed into networks of these slope detectors, which may aid in gas-based navigation tasks^{16,17,21}.

Such robotics applications could be particularly useful in combination with neuromorphic computing. Biophysical neuron models are inherently inefficient to emulate on event-driven neuromorphic hardware. A point neuron model such as the one used in this study requires a minimal set of parameters and only needs to communicate with other neurons in the network upon firing an action potential, therefore fulfilling the criteria of communication sparseness and memory locality that is a prerequisite for efficient operation on fully-distributed neuromorphic computing approaches. Izhikevich models have been successfully employed in various applications on neuromorphic hardware⁹⁻¹¹.

In this light, one area of potential future work is to focus on more complex stimuli. Gas concentration dynamics in a turbulent plume are extremely complex^{2,5}. The Gaussian white noise input signal used in this study is limited in its ability to represent the rich temporal structure encountered in real odour plumes. One opportunity could be to use time series data obtained from real odour plumes in wind tunnels²².

Therefore, the broader impact of this study extends beyond simple bio-mimicry. It supports a paradigm shift in neuromorphic computing, moving towards genuine computing approaches that harness the specific efficiency of employing a neuronal approach, where time is implicitly included in the computation process.

Future research can implement these detectors in various fields of study that require rapid computations and low-latency responses, paving the way for advancements in neuromorphic hardware, gas-based navigation research, robotic platforms, and other domains where efficient neuronal computations are essential.

Method

All simulations were created using PyNN and conducted using the NEURON simulator²³ with the built-in Izhikevich neuron model⁸. In this section, we present the methods employed in our study, including the search of the Izhikevich parameter space and the comparison between the discovered Izhikevich bursting slope detector neuron and the two-compartmental biophysical neuron model¹.

i) Identifying slope and amplitude detectors in the Izhikevich parameter space

We conducted a systematic search of the Izhikevich parameter space to identify sets of parameters that produced either slope or amplitude-detecting neurons. The parameters a , c , and d were explored over a wide range of values. To define the search boundaries, we examined parameters known to produce specific neural behaviours, such as intrinsically bursting or fast-spiking. We fixed parameter b to a value of 0.2 based on previous research and its ability to reproduce desired behaviours. By considering a broad range of parameter values and known neural behaviours, we aimed to comprehensively cover the parameter space and identify parameter sets that produce slope or amplitude-detecting neurons. Simulations were performed on the UH-HPC cluster for efficient computational handling.

In the first instance we injected sinusoidal input signals (rectified, 4 Hz) into each Izhikevich point neuron with the set parameters. The output spike trains were compared to the original input signal. We specifically looked at the spike rate corresponding to the rising edges of the input signal to identify slope detectors and the spike rate corresponding to the peaks of the input signal to identify amplitude detectors. Later, we investigated whether there was a relationship between these detectors and the bursting mechanisms.

The *slope detection percentage* and *amplitude detection percentage* were calculated to find the optimal parameter sets for the strongest detectors. The *slope detection percentage* was calculated by determining the number of spikes that occurred on the slopes of the input signal. For bursting neurons, only burst onsets were considered. This count was then divided by the total number of spikes or burst onsets observed during the simulation. The resulting fraction represents the proportion of spikes or burst onsets that coincided with the rising edges of the input signal. By multiplying this fraction by 100, we obtained the *slope detection percentage*, which provides a quantitative measure of the neuron's ability to detect slopes.

Similarly, *amplitude detection percentage* was calculated by determining the number of spikes that occurred on the peaks of the signal. We then investigated the relationship between bursting behaviour and amplitude or slope detection. Bursting was defined by an inter-spike interval (ISI) of 10 ms. The *burst percentage* was calculated as the percentage of spikes occurring within a burst.

To assess the robustness of the detectors we discovered, Gaussian white noise signals were generated, low-pass filtered using a Butterworth filter (5 Hz; $\mu = .006$; $\sigma = .015$), and injected into the detectors. The ability of the detectors to respond to different input types was evaluated. If these detectors are robust (which we show to be the case), their capabilities should not be restricted to sinusoidal inputs.

ii) Bursting slope detector comparison

We compared the Izhikevich bursting slope detector neuron we discovered to the two-compartmental biophysical neuron model¹. The biophysical neuron model consists of a dendrite compartment responsible for bursting behaviour and a somatic region generating fast spikes. To ensure a fair comparison, we created a robust neuron that demonstrated 100% *slope detection percentage* and 100% *burst percentage*, as identified in our previous investigations.

We conducted a comparison study of the behaviours observed in the biophysical neuron model by generating a Gaussian white noise signal, applying a Butterworth low-pass filter (5 Hz; $\mu = .006$; $\sigma = .015$), and injecting it into the slope-detector we discovered. We investigated how this detector responds to input signals within a range of frequencies. The response of this detector was evaluated using reverse correlation techniques (spike-triggered average) to identify the features of the input signal triggering its response. By aligning the input signal with spike occurrences and averaging across multiple spikes, it reveals the average input signal associated with the detector's spiking activity, providing insights into the specific characteristics driving the detector's response.

iii) Bi-directional slope detection

We investigated whether the slope-detector we discovered was capable of bi-directional slope detection, as demonstrated by the biophysical neuron model¹. We observed whether it could detect positive slopes of the input signals and the down-strokes when inverted.

To examine the excitatory response, we generated a Gaussian white noise signal (5 Hz; $\mu = .008$; $\sigma = .015$) and directly injected it into the detector. The sign of the signal was then inverted to simulate the inhibitory input. The resulting signal was injected into the neuron to observe the inhibitory response. We followed the authors method so we could directly compare the results.

iv) Burst duration encoding

To conclude our comparison studies, we investigated whether the bursts from the bursting slope detector neuron we discovered only marked the occurrence of signal up-strokes or if they also signalled the slope magnitude. We therefore observed the distribution of input slopes against burst durations, i.e., the number of spikes in a burst which was defined by a fixed ISI of 10 ms.

A Kernel Density Estimation (KDE) plot was created to display the number of spikes per burst divided by a Gaussian density estimation, providing the fraction of bursts for different signal slopes. From this, we created a ROC (Receiver Operator Characteristic) curve to observe the discriminability between two burst length distributions and used the composite trapezoidal rule to calculate the AUC (Area Under the Curve) value. An AUC value of 1 indicates perfect discrimination between the two burst length distributions, meaning there is no overlap and the burst length informs the magnitude of the slope.

Author contributions statement

R.M. Methodology, Software, Investigation, Visualization, Writing - Original Draft, Writing - Review and Editing.

Ma.S. Methodology, Writing - Review and Editing, Supervision.

V.S. Conceptualisation, Methodology, Writing - Review and Editing, Supervision.

Mi.S. Conceptualisation, Methodology, Writing - Review and Editing, Supervision, Funding Acquisition.

Funding received from the NSF/MRC NeuroNex Odor2Action programme (NSF #2014217, MRC #MR/T046759/1).

Data availability statement

The datasets generated and/or analysed during the current study are available in the GitLab repository: <https://gitlab.com/r-miko/slope-detector-project>

References

1. Kepecs, A., Wang, X. J. & Lisman, J. Bursting neurons signal input slope. *J. Neurosci.* **22**, 9053–9062, DOI: [10.1523/jneurosci.22-20-09053.2002](https://doi.org/10.1523/jneurosci.22-20-09053.2002) (2002).
2. Celani, A., Villermaux, E. & Vergassola, M. Odor landscapes in turbulent environments. *Phys. Rev. X* **4**, 041015, DOI: [10.1103/PhysRevX.4.041015](https://doi.org/10.1103/PhysRevX.4.041015) (2014).
3. Schmuker, M., Bahr, V. & Huerta, R. Exploiting plume structure to decode gas source distance using metal-oxide gas sensors. *Sensors Actuators, B: Chem.* **235**, 636–646, DOI: [10.1016/j.snb.2016.05.098](https://doi.org/10.1016/j.snb.2016.05.098) (2016).
4. Jacob, V., Monsempès, C., Rospars, J.-P., Masson, J.-B. & Lucas, P. Olfactory coding in the turbulent realm. *bioRxiv* DOI: [10.1101/179085](https://doi.org/10.1101/179085) (2017).
5. Justus, K. A., Murlis, J., Jones, C. & Cardé, R. T. Measurement of odor-plume structure in a wind tunnel using a photoionization detector and a tracer gas. *Environ. Fluid Mech.* **2**, 115 – 142, DOI: [10.1023/a:1016227601019](https://doi.org/10.1023/a:1016227601019) (2002).
6. Szyszka, P., Gerkin, R. C., Galizia, C. G. & Smith, B. H. High-speed odor transduction and pulse tracking by insect olfactory receptor neurons. *Proc. Natl. Acad. Sci.* **111**, 16925–16930, DOI: [10.1073/pnas.1412051111](https://doi.org/10.1073/pnas.1412051111) (2014).
7. Ackels, T. *et al.* Fast odour dynamics are encoded in the olfactory system and guide behaviour. *Nature* **593**, 558–563, DOI: [10.1038/s41586-021-03514-2](https://doi.org/10.1038/s41586-021-03514-2) (2021).
8. Izhikevich, E. M. Simple model of spiking neurons. *IEEE Transactions on Neural Networks* **14**, 1569–1572, DOI: [10.1109/TNN.2003.820440](https://doi.org/10.1109/TNN.2003.820440) (2003).
9. Sapounaki, M. & Kakarountas, A. A novel low-power neuromorphic circuit based on izhikevich model. In *2021 10th International Conference on Modern Circuits and Systems Technologies (MOCASST)*, 1–4, DOI: [10.1109/MOCASST52088.2021.9493396](https://doi.org/10.1109/MOCASST52088.2021.9493396) (2021).
10. Çağdaş, S. & Şengör, N. S. A folded architecture for hardware implementation of a neural structure using izhikevich model. In *International Conference on Artificial Neural Networks*, 508–518, DOI: [10.1007/978-3-031-15934-3_42](https://doi.org/10.1007/978-3-031-15934-3_42) (2022).
11. Dey, S. & Dimitrov, A. Mapping and validating a point neuron model on intel’s neuromorphic hardware loihi. *Front. Neuroinformatics* **16**, 883360, DOI: [10.3389/fninf.2022.883360](https://doi.org/10.3389/fninf.2022.883360) (2022).
12. Zahra, O., Tolu, S. & Navarro-Alarcon, D. Differential mapping spiking neural network for sensor-based robot control. *Bioinspiration & Biomimetics* **16**, DOI: [10.1088/1748-3190/abedce](https://doi.org/10.1088/1748-3190/abedce) (2021).
13. Feng, S., Xu, W., Yao, B., Liu, Z. & Ji, Z. Early prediction of turn-taking based on spiking neuron network to facilitate human-robot collaborative assembly. In *2022 IEEE 18th International Conference on Automation Science and Engineering (CASE)*, 123–129, DOI: [10.1109/CASE49997.2022.9926441](https://doi.org/10.1109/CASE49997.2022.9926441) (IEEE, 2022).
14. Gabbiani, F., Metzner, W., Wessel, R. & Koch, C. From stimulus encoding to feature extraction in weakly electric fish. *Nature* **384**, 564–567, DOI: [10.1038/384564a0](https://doi.org/10.1038/384564a0) (1996).
15. Hodgkin, A. L. & Huxley, A. F. A quantitative description of membrane current and its application to conduction and excitation in nerve. *The J. Physiol.* **117**, 500–544, DOI: [10.1113/jphysiol.1952.sp004764](https://doi.org/10.1113/jphysiol.1952.sp004764) (1952).
16. Miko, R., Steuber, V. & Schmuker, M. Brain-inspired spiking neural network for gas-based navigation. *ECS* **38** (2019).
17. Miko, R., Steuber, V. & Schmuker, M. Replicating bursting neurons that signal input slopes with izhikevich neurons. *BMC Neurosci.* **49**, 160, DOI: [10.1007/s10827-022-00812-0](https://doi.org/10.1007/s10827-022-00812-0) (2021).

18. Drix, D. & Schmuker, M. Resolving fast gas transients with metal oxide sensors. *ACS sensors* **6**, 688–692, DOI: [10.1021/acssensors.0c02006](https://doi.org/10.1021/acssensors.0c02006) (2021).
19. Drix, D., Dennler, N. & Schmuker, M. Rapid recognition of olfactory scenes with a portable mox sensor system using hotplate modulation. In *2022 IEEE International Symposium on Olfaction and Electronic Nose (ISOEN)*, 1–4, DOI: [10.1109/ISOEN54820.2022.9789654](https://doi.org/10.1109/ISOEN54820.2022.9789654) (IEEE, 2022).
20. Dennler, N., Drix, D., Rastogi, S., van Schaik, A. & Schmuker, M. Rapid inference of geographical location with an event-based electronic nose. In *Proceedings of the 2022 Annual Neuro-Inspired Computational Elements Conference*, 112–114, DOI: [10.1145/3517343.3517381](https://doi.org/10.1145/3517343.3517381) (2022).
21. Miko, R., Steuber, V. & Schmuker, M. Determinants of input amplitude and slope detection in bursting neurons. *J. Comput. Neurosci.* P59 (2023).
22. Connor, E. G., McHugh, M. K. & Crimaldi, J. P. Quantification of airborne odor plumes using planar laser-induced fluorescence. *Exp. Fluids* **59**, 1–11, DOI: [10.1007/s00348-018-2591-3](https://doi.org/10.1007/s00348-018-2591-3) (2018).
23. Hines, M. L. & Carnevale, N. T. The neuron simulation environment. *Neural computation* **9**, 1179–1209, DOI: [10.1162/neco.1997.9.6.1179](https://doi.org/10.1162/neco.1997.9.6.1179) (1997).